NUMERICAL SIMULATION OF CAVITATION BUBBLE GROWTH WITHIN A DROPLET

M. Lü Z. Ning * K. Yan J. Fu C.-H. Sun

College of Mechanical and Electrical Engineering
Beijing Jiaotong University
Beijing, P. R. China

ABSTRACT

Cavitation bubbles, which always exist in the diesel jet leaving the nozzle and in diesel droplets breaking up from the jet as a result of supercavitation of the diesel within the injection nozzle, increase the instability of jet and droplets in part due to the two-phase mixture, while the mechanism of this effect is still unclear. Cavitation bubble expansion within the diesel droplet has been simulated numerically based on the volume of fluid (VOF) method, and the control mechanism of bubble growth process is analyzed by Rayleigh-Plesset equation. The process of bubble growth is divided into three parts, including surface tension controlled domain, comprehensive competition controlled domain and inertial force controlled domain. During the first stage, cavitation bubble growth is controlled by the surface tension, and the decrease of the surface tension leads to the increase of the bubble growth rate. During the second stage, the bubble growth rate is controlled by the comprehensive competition of the surface tension, the inertial force and the viscous force. During the third stage, the process of bubble growth is majorly controlled by the inertial force.

Keywords: Droplet, Cavitation bubble, Numerical simulation, Control mechanism.

1. INTRODUCTION

It is well known that cavitation in injection nozzles has a strong impact on spray formation and atomization, which are directly correlated to the efficiency of the combustion process that results in higher performance and modifies pollutant emissions [1,2]. The Cavitation phenomenon in injection nozzles is divided into two types, onset of cavitation and supercavitation [3]. Supercavitation in the process of fuel injection refers to a kind of phenomenon that cavitation bubbles exist in the fuel jet leaving the nozzle. Nowadays, with the increasing of the fuel injection pressure, the cavitation phenomenon in fuel injection process has become very prominent.

An interesting physical question is found in many experimental process that more atomization occurs on the liquid jet with the stronger cavitation [4-9]. For instance, Safari [7], Desantes, *et al* [8], and Payri, *et al* [9] studied the effects of cavitation in a nozzle hole on atomization of spray respectively, and their results reveal that the liquid jet with the stronger cavitation leads to more atomization. However, supercavitation turns the fuel jet into gas-liquid two-phase mixture flow, which increases the instability of fuel jet and has an important impact on the breakup and atomization of fuel injection process so that the spray breakup and atomization mechanism under the condition of supercavitation is still unclear.

Cavitation bubbles, which always exist in the diesel jet leaving the nozzle and in diesel droplets breaking up from the jet as a result of supercavitation of the diesel within the injection nozzle, increase the instability of jet and droplets in part due to the two-phase mixture, while the mechanism and degree of this effect is uncertain. Due to the small scale of diesel droplets and cavitation bubbles, and the high jet speed of several hundred meters per second, experimental studies on the breakup of cavitation bubble within the droplet are very limited.

Actually, studying on the process of cavitation bubble growth is always an important branch of bubble dynamics. The first analysis of this problem in cavitation and bubble dynamics was made by Rayleigh [10], who solved the problem of the collapse of an empty cavity in a large mass of liquid. With neglect of surface tension and liquid viscosity and with the assumption of liquid incompressibility, Rayleigh showed from the momentum equation that the bubble boundary $R(t)$ obeyed the relation [11]

$$R\ddot{R}+\frac{3}{2}\dot{R}^2=\frac{p(R)-p(\infty)}{\rho}, \tag{1}$$

where ρ is the liquid density, $p(\infty)$ is the pressure in the liquid at a large distance from the bubble, and $p(R)$ is

* Corresponding author (zhining@bjtu.edu.cn)

DOI : 10.1017/jmech.2015.57
Copyright © 2015 The Society of Theoretical and Applied Mechanics, R.O.C.
https://doi.org/10.1017/jmech.2015.57 Published online by Cambridge University Press

the pressure in the liquid at the bubble boundary. For this Rayleigh problem, $p(R)$ is also the pressure within the bubble. On the basis of Eq. (1), Plesset [11,12] extended the Rayleigh Equation to include the effects of surface tension and liquid viscosity

$$p(R) = p_{in} - \frac{2\sigma}{R} - \frac{4\mu}{R}\dot{R}, \tag{2}$$

where now p_{in} is the pressure in the bubble and $p(R)$, as before, is the pressure in the liquid at the bubble boundary. The surface tension constant and the coefficient of the liquid viscosity are σ and μ, respectively. Besides, Robinson and Judd [13] studied the growth characteristics of a single isolated spherical bubble expanding in a uniformly superheated unbounded liquid, and they divided the process of bubble growth into three stages, including surface tension controlled domain, transition domain and heat transfer controlled domain. Zhang [14,15] investigated theoretically and numerically the growth and collapse of a bubble in free flow field. Therefore, most research results are obtained by studying on cavitation bubble growth and collapse in a uniformly unbounded liquid flow.

At present, studies on cavitation bubble growth within a droplet are very limited. To our knowledge, these studies are generally carried out by analytical method. Zeng and Lee [16] applied the linear stability analysis method to develop a simple mathematical model to solve the secondary droplet character of dimethyl ether, however, they neglected the viscosity of the DME droplet, the DME bubble and the air surrounding the DME droplet. On the basis of their research results, Lü and Ning [17] considered the effects of fluids viscosities, including droplet, cavitation bubble and surrounding air, and extended Zeng's mathematical model. However, due to the exists of assumed conditions, analytical method cannot be used to reveal more details about cavitation bubble growth within a droplet, which makes it impossible for us to deeply understand the whole growth process of cavitation bubble within a droplet. Also, the control mechanism of bubble growth process is still not clear. Therefore, it is obvious that numerical simulation is very promising to improve the understanding of the growth process and its control mechanism of cavitation bubble within a droplet.

In this paper, cavitation bubble expansion within the diesel droplet has been simulated numerically based on the volume of fluid (VOF) method, and the control mechanism of bubble growth process is analyzed by Rayleigh-Plesset equation. The study is organized as follows. The VOF method, governing equations and numerical method are given in Sec. 2. The solvability conditions and validation of the numerical method are presented in Sec. 3. The results and discussions are presented in Sec. 4, which includes bubble growth process and its control mechanism. Conclusions are given in Sec. 5.

2. VOF METHOD AND GOVERNING EQUATIONS

2.1 VOF Method

The key issue of studying Gas-liquid two-phase flow is to determine the location of phase interface and distribution of the phases. VOF method is a numerical method for solving the gas-liquid two-phase flow and free-surface flows.

VOF method can track the location of phase interface by the use of fluid volume fraction function α and its control equation in each grid cell. The indicator function α can be expressed as:

$$\alpha(x,t) = \begin{cases} 1, & \text{liquid-phase} \\ 0 < \alpha < 1, & \text{gas-liquid two-phase} \\ 0. & \text{gas-phase} \end{cases} \tag{3}$$

For the two-phase flow problem, the fluid properties density, ρ, and dynamic viscosity, μ, depending on the indicator function, α, are defined as:

$$\rho = \alpha_1\rho_1 + \alpha_2\rho_2 \tag{4}$$

$$\mu = \alpha_1\mu_1 + \alpha_2\mu_2 \tag{5}$$

$$\alpha_1 + \alpha_2 = 1 \tag{6}$$

where the subscript 1 and 2, represent fluid 1 and fluid 2 respectively. The interface is then transported using the following advection equation called the ''VOF equation'':

$$\frac{\partial\alpha}{\partial t} + (\mathbf{V}\cdot\nabla)\,\alpha = 0 \tag{7}$$

where **V** represent the fluid velocity.

There are two important problems in using VOF method, interface reconstruction and interface advancing with time. In this paper, the piecewise linear interface calculation (PLIC) method is employed to reconstruct the interface, and the operator non-splitting algorithm is employed to advance the interface with time.

2.2 Governing Equations

This paper presents a preliminary study on the growth of cavitation bubble within a diesel droplet. The research object consists of three parts, the diesel droplet, cavitation bubble within the diesel droplet, and the ambient air, as shown in Fig. 1. It is assumed that the ambient air and the diesel droplet are viscous and incompressible while the cavitation bubble is viscous and compressible. Furthermore, the following assumptions are reasonably made: (1) only one bubble within the droplet, (2) no heat and mass transfer at the interface, and (3) neglecting the effect of gravity.

With the above assumptions, the governing equations for fluid flows can be given as below:

https://doi.org/10.1017/jmech.2015.57 Published online by Cambridge University Press

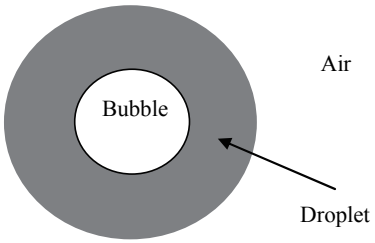


Fig. 1 Schematic of cavitation bubble and droplet.

$$\frac{\mathrm{D}\rho}{\mathrm{D}t}+\rho\nabla\cdot\mathbf{V}=0 \tag{8}$$

$$\rho\frac{\mathrm{D}\mathbf{V}}{\mathrm{D}t}=-\nabla p+\mu\nabla^2\mathbf{V}+\frac{1}{3}\mu\nabla(\nabla\cdot\mathbf{V})+\sigma k\mathbf{n} \tag{9}$$

$$\frac{\partial\alpha_i}{\partial t}+(\mathbf{V}\cdot\nabla)\,\alpha_i=0 \tag{10}$$

$$\frac{\partial p_3}{\partial\rho_3}=c \tag{11}$$

where $\mathbf{V}$ is the fluid velocity, ρ is the fluid density, μ is the dynamic viscosity, p is the fluid pressure, σ is the surface tension coefficient, $\mathbf{n}=\nabla\alpha_i$, is the gradient vector of volume fraction which is perpendicular to the interface, $k=\nabla\cdot(\mathbf{n}/|\mathbf{n}|)$, is the curvature at the interface, c is the constant, the subscript i = 1, 2 and 3, represent the diesel droplet, the ambient air and the cavitation bubble within diesel droplet respectively.

In Eq. (9), the last item of the right hand side reflects the effect of surface tension, which includes the surface tension between the bubble and droplet and the surface tension between the droplet and air. The surface tension is calculated by using continuous surface tension model (CSF model). Take the surface tension between the bubble and droplet $\mathbf{F}$ for example, $\mathbf{F}$ is defined as:

$$\mathbf{F}=\sigma k\mathbf{n}=\sigma\nabla\cdot\left(\frac{\nabla\alpha_1}{|\nabla\alpha_1|}\right)\nabla\alpha_1 \tag{12}$$

2.3 Numerical Method

The governing equations presented above are solved using the finite volume CFD code OpenFOAM. A second-order Crank-Nicholson scheme is used to discretize the temporal terms, and a second-order Gauss linear scheme is used to discretize the gradient derivative terms such as ∇p. Considering a step on both sides of the phase interface, we use Gauss van Leer scheme to discretize the convection divergence term in Eq. (10). The other convection divergence terms are discretized by second-order Gauss upwind scheme. A second-order Gauss linear corrected scheme is used to discretize the Laplacian terms. The solution procedure employs the PISO (Pressure Implicit with Splitting of Operators) algorithm, used for transient problems.

3. SOLVABILITY CONDITIONS AND VERIFICATION

3.1 Computational Domain and Solvability Conditions

Physical parameters of the diesel droplet, air and cavitation bubble are set at the temperature of 300K according to the Ref. [18-20], and the parameters in the calculation are shown in Table 1.

As the research object consists of three parts, the diesel droplet, cavitation bubble within the diesel droplet, and the ambient air are included into the computational domain. Since the research object is axisymmetric, and what we concern is just the change of the diameter, so our issues can be reduced into a two-dimensional problem and we solve the equations in two-dimensions. In addition, for bubble growth process, rectangular mesh can make every mesh cells equal easily, while polar mesh does not make it dense internal cells and sparse outside cells. Therefore, rectangular mesh is more appropriate than polar mesh. At last, the computational region is taken as a square, 0.2mm × 0.2mm. The inner region is the cavitation bubble, the middle region is the diesel droplet, and the outer region is air. The initial radius of the cavitation bubble is 5μm, and the initial radius of the diesel droplet is 10μm, as shown in Fig. 2.

Buoyant pressure condition is used in outlet boundary, and zero gradient velocity setup. Fluids are free access to the outlet boundary. The initial pressure of the cavitation bubble is set to 9×10^5 Pa, the initial pressure of the diesel droplet is set to 1×10^5 Pa, and the initial pressure of the ambient air is set to 1×10^5 Pa.

In addition, the time step should be set before the numerical calculation. Setting the time step is classified into the constant time step and automatic adjustment of the time step. Setting the constant time step is relatively simple, and we just need to meet the requirements of the stability of discretization schemes (Courant number Co < 1). However, constant time step may waste the computation time in the unsteady flows. In view of this, we set the time step as automatic adjustment of the time step, the initial value of time step as 2×10^{-8}s, and the maximum Co for phase fields as 0.25.

The calculated region is splitted by structured grid. The grid independence analysis has been performed, then we set the grid numbers as 400 × 400 and mesh size as 2.50×10^{-13}m^2.

3.2 Numerical Validation

In order to verify the correctness of the numerical method proposed in this paper, the bubble collapse in a uniformly unbounded liquid flow has been investigated numerically, and compared with the original data in the literature [10] and [15], as shown in Fig. 3. Rayleigh [10] gives the analytical results about the collapse of an empty cavity in a large mass of liquid. Zhang [15] gives the numerical results of the collapse of a bubble in free flow field. As shown in Fig. 3,

https://doi.org/10.1017/jmech.2015.57 Published online by Cambridge University Press

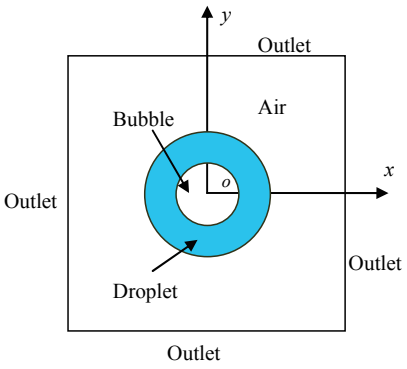


Fig. 2 Schematic of computational domain.

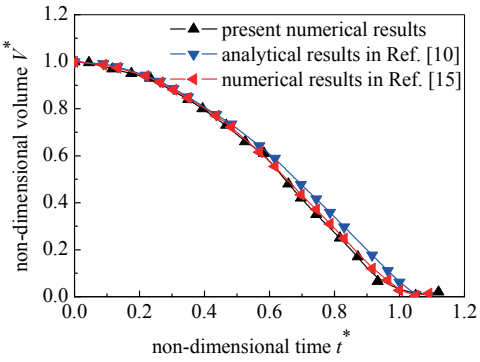


Fig. 3 Comparison of the calculation results of bubble collapse with the data in the literature [10] and [15].

Non-dimensional bubble volume V^* and non-dimensional time t^* are non-dimensionalized by the initial bubble volume V_0 and Rayleigh collapse time t_0 [15] respectively. Also, the calculation results obtained by the numerical method proposed in this paper agree well with the original data from Zhang [15], which suggests that the numerical method is correct. Due to the neglect of surface tension and liquid viscosity in Ref. [10], there are some deviations between analytical results and numerical results.

In addition, Fig. 4 shows that the comparison of present numerical results with analytical results of bubble growth within a diesel droplet in Ref. [17]. By assuming the disturbance at the interface is symmetry, and the perturbation amplitude increased exponentially, Ref. [17] applied the linear stability analysis method to develop a mathematical model to solve the bubble growth and breakup within a diesel droplet. The comparison results consist of two cases: Case 1, bubble 5μm, droplet 10μm; case 2, bubble 5μm, droplet 6.25μm.

As shown in Fig. 4, for case 2, the present numerical results agree well with the analytical results. As for case 1, the present numerical results agree with the analytical results at the beginning, however, when the bubble growth time reaches 1μs, the bubble radius with present numerical result is significantly larger than the one with analytical results. The assumed conditions in analytical method, for instance, the initial disturbance is assumed to be proportional to the initial droplet radius, and the perturbation amplitude is assumed to increase

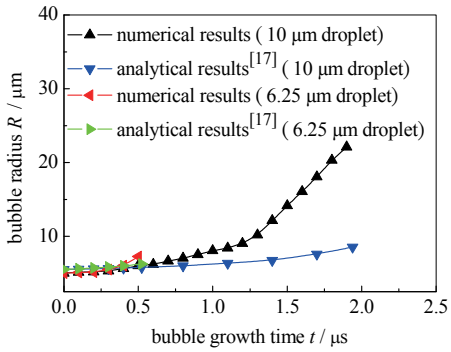


Fig. 4 Comparison of numerical results of bubble (5μm) growth with analytical results [17].

Exponentially, are the reason to make this difference. Therefore, numerical simulation can be used to reveal more details about cavitation bubble growth within a droplet.

4. RESULTS AND DISCUSSIONS

4.1 The Growth Process of Cavitation Bubble Within a Droplet

In order to visualize the growth process of cavitation bubble within a diesel droplet, Fig. 5 represents the phase distribution of bubble and droplet at different times. As shown in Fig. 5, for the given calculation parameters (see Table 1), the variation of bubble radius has some rules to follow. Within the first 0.3μs, the radius change of the bubble within a droplet is smaller, the change of bubble radius is increasingly obvious between 0.3μs and 1.2μs, and the increase of bubble radius is more significant after 1.2μs, then the bubble breakups at about 2.0μs.

Figure 6 illustrates the growth characteristics of cavitation bubble within a diesel droplet, including the variation of bubble radius, velocity and acceleration.

As shown in Fig. 6(a), the variation of bubble radius with time can be divided into three different growth stages: Slow (I), medium (II) and urgent (III).

In stage I, the rate of bubble expansion is lower than 2m/s. In stage II, the bubble expansion rate has increased to 3 ~ 6m/s. In stage III, the bubble expansion rate rapidly increases to 20m/s or so, after a period of time, the bubble expansion rate increases again to the breakup. As represented in Fig. 6(b).

In addition, the variation of bubble acceleration with time also reflects the three different growth stages, as shown in Fig. 6(c). During the first stage, bubble growth acceleration is less than 15m/s^2. During the second stage, bubble growth acceleration has increased, and the maximum acceleration is about 30m/s^2. During the third stage, bubble growth acceleration can be up to 80m/s^2 or so.

https://doi.org/10.1017/jmech.2015.57 Published online by Cambridge University Press

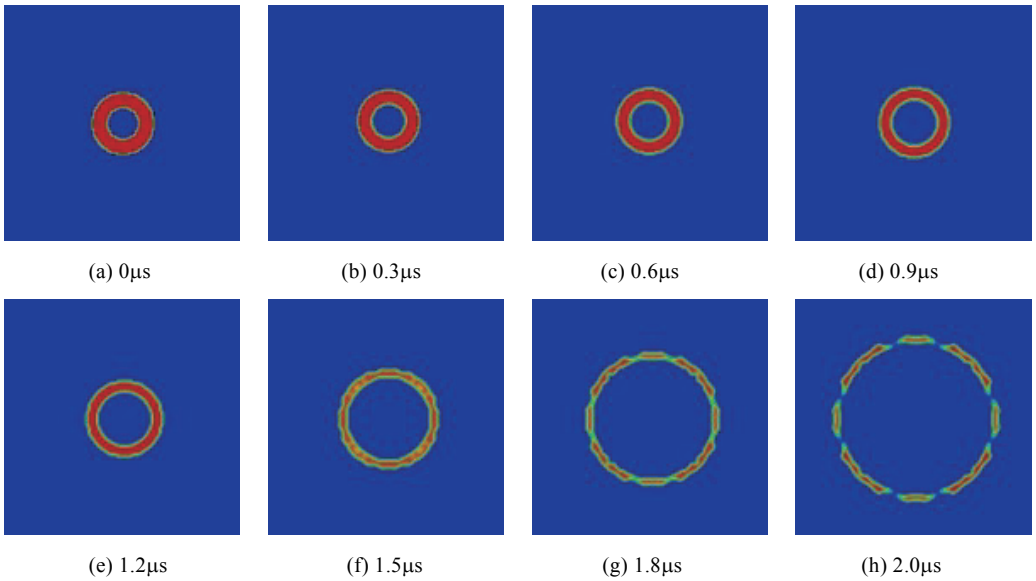


Fig. 5 Phase distribution versus time.

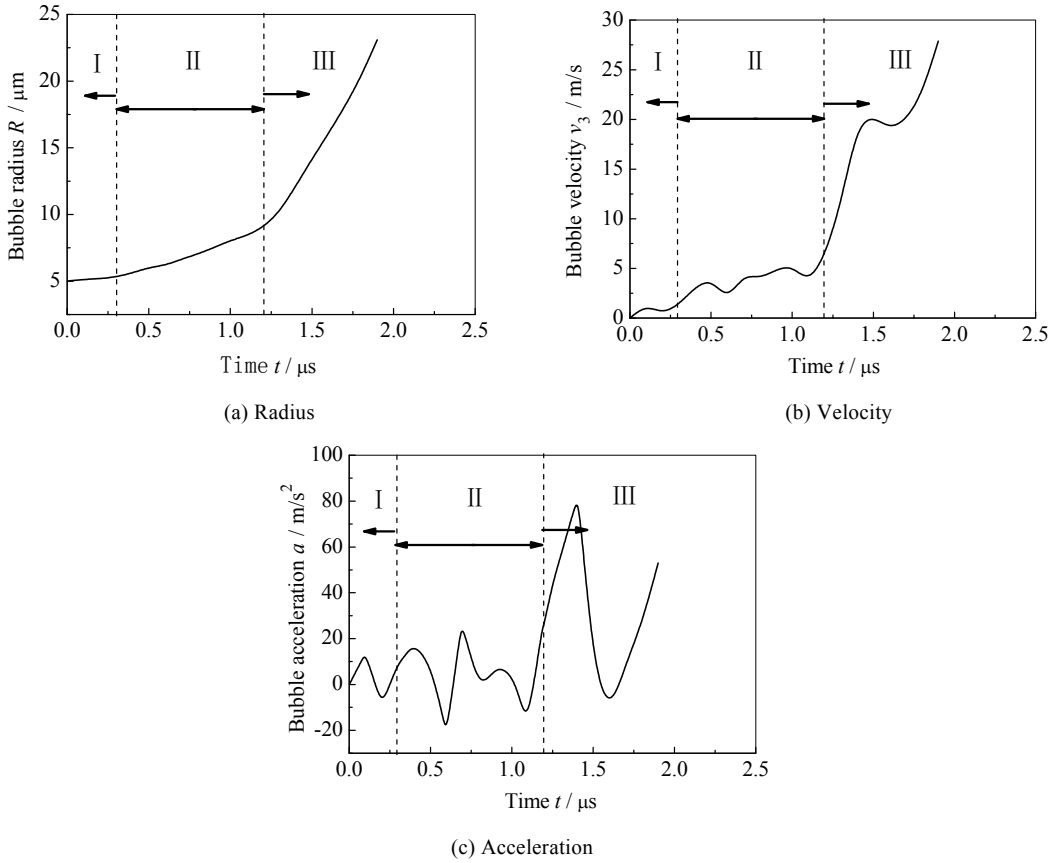


Fig. 6 Growth characteristics of cavitation bubble within a diesel droplet.

4.2 The Control Mechanism of Bubble Growth

In the following section, the control mechanism of bubble growth process will be discussed by the present numerical results and Rayleigh-Plesset equation.

Rayleigh-Plesset equation can be represented by [12]:

$$p_3 - p(R) = \frac{2\sigma}{R} + \rho_1 R\frac{\mathrm{d}^2 R}{\mathrm{d}t^2} + \frac{3}{2}\rho_1\left(\frac{\mathrm{d}R}{\mathrm{d}t}\right)^2 + \frac{4\mu_1}{R}\frac{\mathrm{d}R}{\mathrm{d}t} \quad (13)$$

where p_3 is the pressure in the bubble, $p(R)$ is the pressure in the liquid at the bubble boundary, σ is the surface tension coefficient, ρ_1 is the diesel liquid density, μ is the dynamic viscosity of the diesel liquid, R is the bubble radius.

https://doi.org/10.1017/jmech.2015.57 Published online by Cambridge University Press

Table 1 Summary of physical parameters.

Parameters	Value
Diesel density / (kg·m^{-3})	848
Diesel viscosity / (Pa·s)	2.936×10^{-3}
Surface tension coefficient / (N·m^{-1})	2.689×10^{-2}
Air density / (kg·m^{-3})	1.193
Air viscosity / (Pa·s)	1.845×10^{-5}
Cavitation gas viscosity / (Pa·s)	1.81×10^{-6}
Bubble radius / (m)	5×10^{-6}
Diesel droplet radius / (m)	1×10^{-5}

The first term $2\sigma/R$ in the right of Eq. (13) arises from the capillary effect, which is inhibiting the growth of cavitation bubble within a droplet. The second and third terms, $\rho_l R\frac{\mathrm{d}^2R}{\mathrm{d}t^2}+\frac{3}{2}\rho_l\left(\frac{\mathrm{d}R}{\mathrm{d}t}\right)^2$, in the right of Eq. (13) arise from the inertial force, which represent the promoting effect by inertial force on the bubble growth within a droplet. The fourth term $\frac{4\mu_l}{R}\frac{\mathrm{d}R}{\mathrm{d}t}$ in the right of Eq. (13) arises from the viscous force, which represents the inhibiting effect on bubble growth. Therefore, Eq. (13) indicates that the pressure difference which dominates the bubble growth is majorly influenced by three forces, including surface tension, inertial force and viscous force.

Figure 7 represents the three forces acting on cavitation bubble versus time in the process of cavitation bubble within a droplet.

As shown in Fig. 7, during the first stage of bubble growth, the surface tension acting on the bubble-liquid interface is greater than 10kN/m^2 and declines as a small rate with time, the inertial force acting on the bubble-liquid interface is approximately zero, and the viscous force is less than 3kN/m^2. Therefore, cavitation bubble growth is controlled by the surface tension in stage I, the decrease of the surface tension leads to the increase of the bubble growth rate, and the inertial force acting on the bubble-liquid interface and the viscous force are insignificant.

In addition, during the second stage of bubble growth, the surface tension decreases gradually from 10kN/m^2 to about 6kN/m^2, the inertial force fluctuates between 1kN/m^2 and 16kN/m^2, and the viscous force changes in 3 ~ 8kN/m^2, shown in Fig. 7. Therefore, cavitation bubble growth is affected simultaneously by three forces in stage II, and the bubble growth rate is controlled by the comprehensive competition of the surface tension, the inertial force and the viscous force.

During the third stage, the surface tension is reduced to 6kN/m^2 or less, the maximum viscous force is less than 20kN/m^2, while the inertial force is almost greater than 50kN/m^2. Therefore, the process of bubble growth is majorly controlled by the inertial force in stage III, the sharp increase of the bubble growth rate stems from the rapid increase of the inertial force, and the surface tension and the viscous force are insignificant.

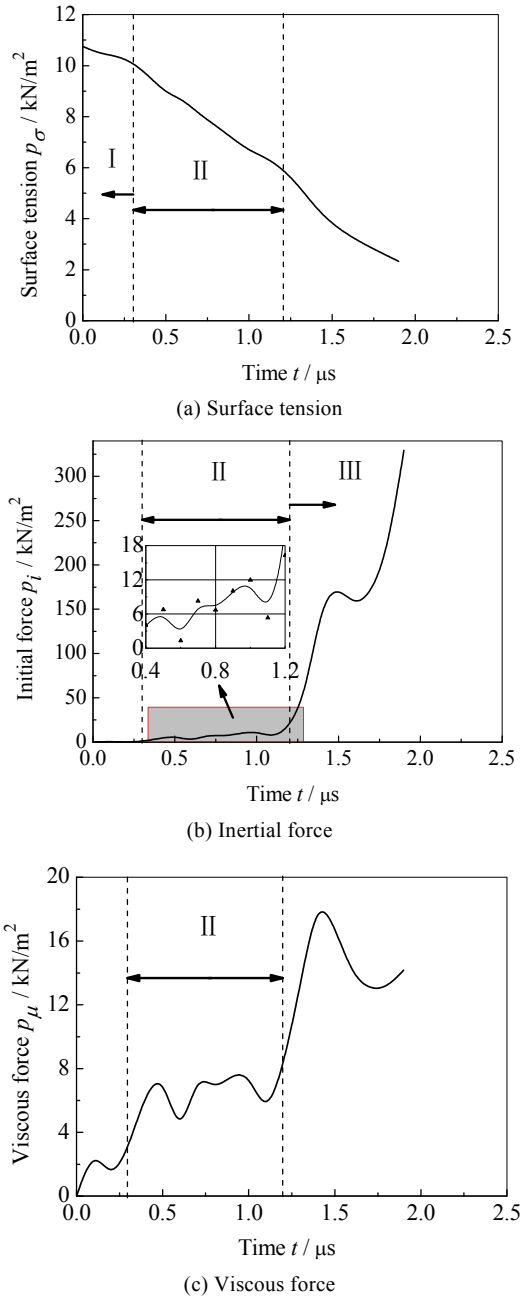


Fig. 7 Forces acting on cavitation bubble versus time.

5. CONCLUSIONS

In this paper, cavitation bubble expansion within the diesel droplet has been simulated numerically based on the volume of fluid (VOF) method, and the control mechanism of bubble growth process is analyzed by Rayleigh-Plesset equation. The process of bubble growth is divided into three parts, including surface tension controlled domain, comprehensive competition controlled domain and inertial force controlled domain. During the first stage, cavitation bubble growth is controlled by the surface tension, and the decrease of the surface tension leads to the increase of the bubble growth rate. During the second stage, cavitation bubble growth is affected simultaneously by three forces, and the bubble growth rate is controlled by the com-

https://doi.org/10.1017/jmech.2015.57 Published online by Cambridge University Press

prehensive competition of the surface tension, the inertial force and the viscous force. During the third stage, the process of bubble growth is majorly controlled by the inertial force, and the sharp increase of the bubble growth rate stems from the rapid increase of the inertial force.

ACKNOWLEDGEMENTS

This project was supported by National Natural Science Foundation of China (51276011), the National High Technology Research and Development Program of China (2013AA065303), Beijing Municipal Natural Science Foundation of China (3132016), and the National High Technology Research and Development Program of China (2011AA11A103-4-1).

REFERENCES

1. Sarre, C. K., Kong, S. C. and Reitz, R. D., "Modeling the Effects of Injector Nozzle Geometry on Diesel Sprays," *SAE Paper*, 1999-01-0912 (1999).
2. Yuan, W. and Schnerr, G. H., "Numerical Simulation of Two-Phase Flow in Injection Nozzles: Interaction of Cavitation and External Jet Formation," *Journal of Fluids Engineering*, **125**, pp. 963–969 (2003).
3. Payri, R., Garcia, J. M. and Salvador, F. J., *et al*, "Using Spray Momentum Flux Measurements to Understand the Influence of Diesel Nozzle Geometry on Spray Characteristics," *Fuel*, **84**, pp. 551–561 (2005).
4. Sou, A., *et al*, "Cavitation in a Two-Dimensional Nozzle and Liquid Jet Atomization," *JSME International Journal*, **49**, pp. 1253–1259 (2006).
5. Sou, A., Hosokawa, S. and Tomiyama, A., "Effects of Cavitation in a Nozzle on Liquid Jet Atomization," *International Journal of Heat and Mass Transfer*, **50**, pp. 3575–3582 (2007).
6. Suh, H. K. and Lee, C. S, "Effect of Cavitation in Nozzle Orifice on the Diesel Fuel Atomization Characteristics," *International Journal of Heat and Fluid Flow*, **29**, pp. 1001–1009 (2008).
7. Safari, S. D., "Effects of Cavitation on High-Pressure Atomization," Ph.D. Dissertation, University of California, Irvine, U.S.A. (2009).
8. Desantes, J. M., *et al*, "Influence of Cavitation Phenomenon on Primary Break-Up and Spray Behavior at Stationary Conditions," *Fuel*, **89**, pp. 3033–3041 (2010).
9. Payri, R, *et al*, "Study of Cavitation Phenomena Based on a Technique for Visualizing Bubbles in a Liquid Pressurized Chamber," *International Journal of Heat and Fluid Flow*, **30**, pp. 768–777 (2009).
10. Rayleigh, L., "On the Pressure Developed in a Liquid During the Collapse of a Spherical Cavity," *Philosophical Magazine*, **34**, pp. 94–98 (1917).
11. Plesset, M. S. and Calif, P., "The Dynamics of Cavitation Bubbles," *ASME Journal of Applied Mechanics*, **16**, pp. 228–231 (1949).
12. Plesset, M. S. and Prosperetti, A., "Bubble Dynamics and Cavitation," *Annual Review of Fluid Mechanics*, **9**, pp. 145–185 (1977).
13. Robinson, A. J. and Judd, R. L., "The Dynamics of Spherical Bubble Growth," *International Journal of Heat and Mass Transfer*, **47**, pp. 5101–5113 (2004).
14. Zhang, L. X., Yin, Q. and Shao, X. M., "Theoretical and Numerical Studies on the Bubble Collapse in Water," *Journal of Hydrodynamics*, **27**, pp. 68–73 (2012).
15. Zhang, L. X., Wen, Z. Q. and Shao, X. M., "Investigation of Bubble-Bubble Interaction Effect During the Collapse of Multi-Bubble System," *Chinese Journal of Theoretical and Applied Mechanics*, **45**, pp. 861–867 (2013).
16. Zeng, Y., "Modeling of Multicomponent Fuel Vaporization in Internal Combustion Engines," Ph.D. Dissertation, University of Illinois, Urbana-Champaign, U.S.A. (2000).
17. Lü, M., *et al*, "The Breakup of Cavitation Bubbles Within the Diesel Droplet," *Chinese Journal of Mechanical Engineering*, **27**, pp. 198–204 (2014).
18. Mulemane, A., *et al*, "Comparing Cavitation in Diesel Injectors Based on Different Modeling Approaches," *SAE Paper*, 2004-01-0027 (2004).
19. Jia, M., *et al*, "A Micro-Variable Circular Orifice Fuel Injector for HCCIConventional Engine Combustion — Part I Numerical Simulation of Cavitation," *SAE Paper*, 2007-01-0249 (2007).
20. Wang, X. and Su, W. H., "A Numerical Study of Cavitating Flows in High-Pressure Diesel Injection Nozzle Holes Using a Two-Fluid Model," *Chinese Science Bulletin*, **54**, pp. 1655–1662 (2009).

(Manuscript received November 21, 2014,
accepted for publication May 25, 2015.)

https://doi.org/10.1017/jmech.2015.57 Published online by Cambridge University Press